



Quantitative evaluation of the tracer distribution in dopamine transporter SPECT for objective interpretation

Yu Iwabuchi¹ · Tadaki Nakahara¹ · Masashi Kameyama^{1,2} · Yoshitake Yamada¹ · Masahiro Hashimoto¹ · Yuji Ogata¹ · Yohji Matsusaka¹ · Mari Katagiri¹ · Kazunari Itoh¹ · Takashi Osada³ · Daisuke Ito³ · Hajime Tabuchi⁴ · Masahiro Jinzaki¹

Received: 14 February 2018 / Accepted: 9 April 2018 / Published online: 13 April 2018
© The Japanese Society of Nuclear Medicine 2018

Abstract

Purpose Quantification of the tracer distribution would add objectivity to the visual assessments of dopamine transporter (DAT) single photon emission computed tomography (SPECT) data. Our study aimed to evaluate the diagnostic utility of fractal dimension (FD) as a quantitative indicator of tracer distribution and compared with the conventional quantitative value: specific binding ratio (SBR). We also evaluated the utility of the combined index SBR/FD (SBR divided by FD).

Materials and methods We conducted both clinical and phantom studies. In the clinical study, 150 patients including 110 patients with Parkinsonian syndrome (PS) and 40 without PS were enrolled. In the phantom study, we used a striatal phantom with the striatum chamber divided into two spaces, representing the caudate nucleus and putamen. The SBR, FD, and SBR/FD were calculated and compared between datasets for evaluating the diagnostic utility. Mann–Whitney test and receiver-operating characteristics (ROC) analysis were used for analysis.

Results ROC analysis revealed that the FD value had high diagnostic performance [the areas under the curve (AUC)=0.943] and the combined use of SBR and FD (SBR/FD) delivered better results than the SBR alone (AUC, 0.964 vs 0.899; $p < 0.001$). The sensitivity, specificity, and accuracy, respectively, were 79.1, 85.0, and 80.7% with SBR, 84.5, 97.5, and 88.0% with FD, and 92.7, 87.5, and 91.3% with SBR/FD.

Conclusion Our results confirmed that the FD value is a useful diagnostic index, which reflects the tracer distribution in DAT SPECT images. The combined use of SBR and FD was more useful than either used alone.

Keywords ¹²³I-Ioflupane · ¹²³I-FP-CIT · DAT · Fractal analysis · Fractal dimension

Abbreviations

PD	Parkinson's disease	DLB	Dementia with Lewy body
PET	Positron emission tomography	SBR	Specific binding ratio
SPECT	Single photon emission computed tomography	VOI	Volume of interest
DAT	Dopamine transporter	FD	Fractal dimension
PS	Parkinsonian syndrome	3D-FA	Three-dimensional-fractal analysis
		NPS	Non Parkinsonian syndrome
		RI	Radioisotope
		OSEM	Ordered-subset expectation maximization
		ICC	Intra-class correlation coefficient
		ROC	Receiver-operating characteristics
		AUC	Area under the ROC curve
		LOA	Limit of agreement
		SSRI	Selective serotonin reuptake inhibitor

✉ Tadaki Nakahara
nakahara@rad.med.keio.ac.jp

¹ Department of Diagnostic Radiology, Keio University School of Medicine, 35 Shinanomachi, Shinjyuku-ku, Tokyo 160-8582, Japan

² Department of Diagnostic Radiology, Tokyo Metropolitan Geriatric Hospital and Institute of Gerontology, Tokyo, Japan

³ Department of Neurology, Keio University School of Medicine, Tokyo, Japan

⁴ Department of Neuropsychiatry, Keio University School of Medicine, Tokyo, Japan

Introduction

A pathophysiological hallmark of Parkinson's disease (PD) is the progressive degeneration of dopaminergic neurons in the substantia nigra. Positron emission tomography (PET) or single photon emission computed tomography (SPECT) with radioactive tracers that have a high affinity for the dopamine transporter (DAT) are regarded as adjuncts to confirm the clinical diagnosis of extrapyramidal diseases. Previous studies have proved that DAT SPECT with ^{123}I -Ioflupane is effective in differentiating neurodegenerative Parkinsonian syndrome (PS) including PD or dementia with Lewy body (DLB) from other neurological disorders such as essential tremor, drug-induced Parkinsonism, and Alzheimer's disease [1, 2].

Visual interpretation plays an important role in assessing DAT SPECT data. The normal striatum is clearly visible as symmetric, comma-shaped regions, with both the caudate and putamen yielding high intensity in images compared to the background, while an asymmetric, dot shaped, or diffuse deterioration pattern is observed in patients with PS. This reflects the fact that the dopaminergic activity in the posterior side of the striatum can be easily compromised owing to disease progression [3] and the tracer accumulation declines from the posterior part of the striatum. Therefore, visual interpretation is thought to be essential, although a previous study indicated that suboptimal inter-observer agreement may lead to variable interpretation of DAT SPECT images [4].

Quantification of striatal uptake is usually conducted in addition to visual assessments of the DAT SPECT images. The quantitative technique is particularly useful for objective evaluation or for the detection of subtle reductions in tracer uptake, which are difficult to capture with visual assessments. Specific binding ratio (SBR), which was proposed by Tossici-Bolt et al. [5], is widely used to measure the total striatal ^{123}I -Ioflupane uptake. This method provides a reproducible and sensitive index using a pentagonal prism-shaped volume of interest (VOI), which encompasses a wide area of the striatum while reducing partial volume effect. However, it is known that the SBR is reduced with aging [6], and that it is affected by the dilatation of the ventricles or the cerebral sulcus [7], leading to inaccurate results in such cases.

Quantifying the information of tracer distribution would make visual interpretation objective. Fractal dimension (FD) is a mathematical index for the quantification of spatial heterogeneity, which can be applied not only to structure but also to tracer distribution, and we construed that FD could enable an objective assessment and replace visual interpretation. Nagao et al. proposed three-dimensional-fractal analysis (3D-FA) to calculate the FD in

SPECT imaging [8–13]. In this method, threshold values of the maximal pixel radioactivity of the SPECT image are set, and the number of pixels obtained at each threshold is measured. FD is calculated on the basis of the relationship between the threshold values and the number of pixels. Figure 1 is the schematic diagram of case with PS and non Parkinsonian syndrome (NPS) when applying 3D-FA to DAT SPECT. We expected that the FD values would increase in cases with PS, because their posterior striatal uptake declines, while cases with NPS show homogeneous radioisotope (RI) distribution.

Furthermore, we can combine SBR and FD quantitatively to obtain the information on tracer accumulation and distribution simultaneously. Previous reports have indicated that a combined approach of visual interpretation and quantitative assessments yields better reproducibility with results and accurate diagnoses [14–17]. Therefore, higher diagnostic ability is expected by combining these two types of quantitative values.

This study aimed to evaluate the utility of FD as a quantitative index of tracer distribution for assessments of DAT SPECT data.

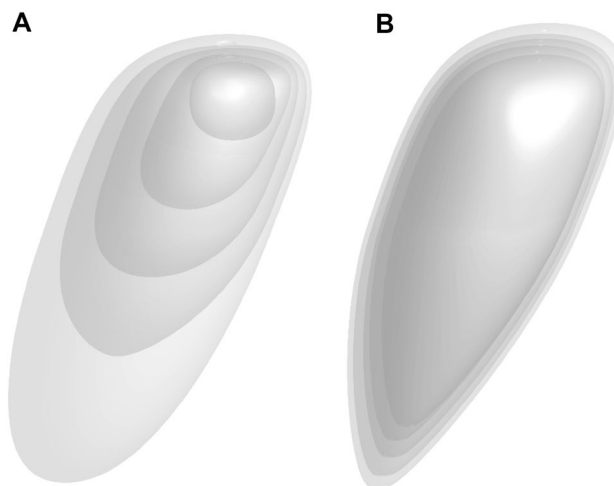


Fig. 1 The schematic diagram of 3D-FA in DAT SPECT: **a** PS pattern; and **b** NPS pattern. For calculating FD value, we changed the threshold so as to delineate the striatum from 40 to 60% of the maximal pixel radioactivity. FD value indicates the transition of the number of pixels according to the change of the threshold setting. In the case of NPS, the transition is not so large, because the RI uptake in the striatum is uniformly high. On the other hand, in the case of PS, the transition becomes larger, because the RI uptake in the striatum is ununiformly low. 3D-FA three-dimensional-fractal analysis, DAT dopamine transporter, SPECT single photon emission computed tomography, PS Parkinsonian syndrome, NPS non Parkinsonian syndrome, FD fractal dimension, RI radioisotope

Materials and methods

Quantification of the SBR, FD, and SBR/FD values

We used two diagnostic indices, SBR and FD, for the quantitative assessments. The SBR was calculated using the DaT-VIEW software (Nihon Medi-Physics, Tokyo, Japan) based on Tossici-Bolt's method [5]. The FD, which represents the spatial distribution of tracer uptake, was calculated using the 3D-FA method proposed by Nagao et al. [8–13]. The 3D-FA method is a modified box counting method of fractal theory. The relationship between a measure (M) and the scale (ϵ) is expressed as,

$$M(\epsilon) = k\epsilon^{-D}, \quad (1)$$

$$\log M(\epsilon) = \log k - D \log \epsilon, \quad (2)$$

where M is the number of pixels within the VOI, ϵ is the threshold value, k is a scaling constant, and D is the fractal dimension.

We set the threshold values so as to delineate the striatum at 40, 45, 50, 55, and 60% of the maximal pixel radioactivity within the VOIs. This threshold setting effectively covers the tracer accumulation of the striatum. In this method, we used the same shape as the Tossici-Bolt's VOI, which encompasses the entire striatal uptake and the partial volume counts detected outside the physical volume of the striatum. Furthermore, we measured the number of pixels within the delineated VOIs obtained at each cut-off level using the ImageJ (National Institutes of Health, Bethesda, MD) software [18]. The number of pixels and the threshold values were transformed into natural logarithms and the relationship between these was plotted to obtain the FD from the slope of the regression line (Fig. 2).

Furthermore, we proposed a more accurate diagnosis, with the introduction of a combination value defined as SBR divided by FD (SBR/FD).

Striatal phantom study

We used a striatal phantom (NMP Business Support Company, Hyogo, Japan) with the striatum chamber divided into two spaces, representing the caudate nucleus and putamen. The ^{123}I concentration was adjusted to be 44 kBq/mL in the caudate nucleus chamber, 44 kBq/mL in the putamen chamber, and 5.5 kBq/mL in the background; thus, their relative proportion was 8:8:1 in the right striatum. The ^{123}I concentration was adjusted to 44, 38.5, and 5.5 kBq/mL, respectively, with a relative proportion of 8:7:1 in the left striatum. We also used relative proportions of 8:6:1, 8:4:1, 8:8:2, 8:7:2, 8:6:2, and 8:4:2, prepared in the same way as described above.

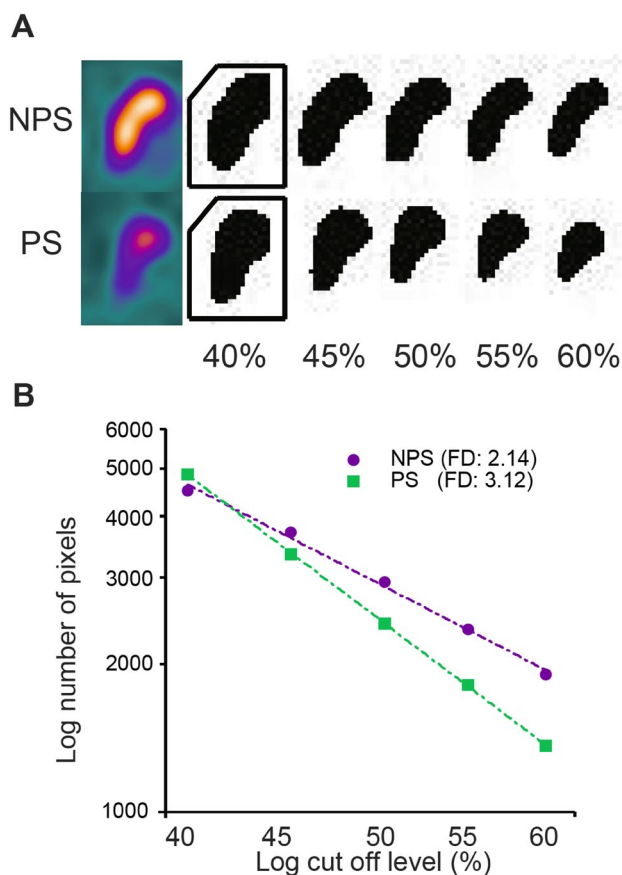


Fig. 2 Representative cases with NPS and PS. FD value can differentiate between NPS and PS cases. *PS* Parkinsonian syndrome, *NPS* non Parkinsonian syndrome, *FD* fractal dimension

Clinical study

In this retrospective study, we selected 183 consecutive patients, who underwent DAT SPECT from February 2014 to August 2015. DAT SPECT was performed to detect abnormalities in the nigrostriatal dopaminergic system. Of the 183 patients, 33 were excluded from the study because of insufficient clinical information, or the effect of some deficiency including infarction or hemorrhage confirmed by CT or MRI images. The remaining 150 patients (median age 68 years; range 30–89 years; male/female, 82/68), including 110 patients with PS and 40 without (NPS), were included.

The patients with PS were diagnosed on the basis of the clinical diagnostic criteria of the UK Parkinson's disease society brain bank (Step1). The 110 patients presented with symptoms of bradykinesia in addition to at least one of the following: muscular rigidity, 4–6 Hz rest tremor, or postural instability, not caused by primary visual, vestibular, cerebellar, or proprioceptive dysfunction. The remaining 40 patients were

diagnosed as NPS, as they did not satisfy the criteria. DLB patients without Parkinsonism were not included in our study.

The institutional review board of the hospital granted permission for this retrospective review of imaging and clinical data, and waived the requirement for obtaining informed consent from the patients.

SPECT acquisition and reconstruction

SPECT imaging was performed using the Discovery NM/CT 670 pro system (GE Healthcare, Milwaukee, WI, USA) mounted with a FAN beam collimator. In the clinical studies, SPECT images were acquired 3 h after the injection of ^{123}I -Ioflupane (185 MBq). The imaging parameters were as follows: matrix size, 128×128 ; pixel size, 4.4 mm; slice thickness, 4.4 mm; energy window, $159 \text{ keV} \pm 10\%$. The projection data acquired for 30 min were reconstructed on a Xeleris workstation (GE Healthcare) using the ordered-subset expectation maximization (OSEM) method (iterations, 3; subset, 10). A Butterworth filter with a critical frequency of 0.5 and power of 10.0 was applied. Neither scatter correction nor attenuation correction was used.

Statistical analysis

All the statistical analyses were performed using the SPSS software (version 14.0J; SPSS Inc., Chicago, IL, USA) and statistical package R (version 3.2.2; available as a free download from <http://www.r-project.org>).

Two nuclear medicine physicians set the VOIs for the calculations of intra-class correlation coefficient (ICC) and for the Bland–Altman analysis [19], for the 150 cases.

The Mann–Whitney test was used to compare values between the two groups. In addition, we performed a receiver-operating characteristics (ROC) analysis of the three indices (SBR, FD, and SBR/FD) to evaluate the area under the ROC curve (AUC). We used the DeLong method for the calculation of the difference between two AUCs [20]. The optimal cut-off values were determined on the basis of the ROC curves, and the sensitivity, specificity, and accuracy of the respective diagnostic values were calculated.

In the clinical study, we measured bilateral striatal uptake of the patients, and the values of worse side were used for statistical analysis.

Results with p values < 0.05 were considered statistically significant.

Results

Striatal phantom study

Figure 3a shows the phantom images of the eight progressively decreasing concentrations used in this study, 8:8:1, 8:7:1, 8:6:1, 8:4:1, 8:8:2, 8:7:2, 8:6:2, and 8:4:2.

We calculated the FD and SBR values from these phantom images and confirmed that the FD values exhibited fractal properties, as linear regression fit values (r^2) of 0.9 or greater were observed in the log–log plots of the total number of pixels vs the threshold values.

The phantom study highlighted the expected relationship between FD and SBR; low concentration of striatal uptake led to a high FD value and a low SBR value (Fig. 3b). In addition, it was proved that FD could detect both, dot and diffuse deterioration patterns; FD tended to increase with a decrease in the RI concentration in the posterior side of the striatum, and FD values of images with the same background concentration were relatively lower than those of images with twice the background concentration.

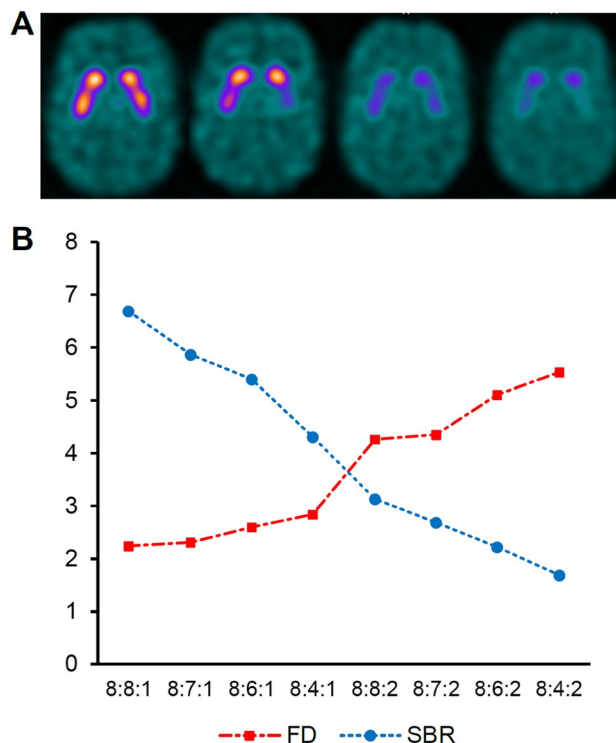


Fig. 3 **a** Phantom images for the 8 types of RI concentration; 8:8:1, 8:7:1, 8:6:1, 8:4:1, 8:8:2, 8:7:2, 8:6:2, and 8:4:2. **b** The FD and SBR values calculated from the phantom images. SPECT single photon emission computed tomography, RI radioisotope, SBR specific binding ratio, FD fractal dimension

Table 1 Patient characteristics

	ALL	PS	NPS	<i>P</i> value
Number of cases	150	110	40	–
Age (years, mean \pm SD)	68 \pm 11.1	69 \pm 10.0	66 \pm 13.5	0.21*
Men/women (<i>N</i>)	82/68	59/51	23/17	0.67 [†]

No significant differences were seen with respect to age and the sex ratio between PS and NPS groups

PS Parkinsonian syndrome, NPS non Parkinsonian syndrome

*ANOVA test

[†]Chi square test

Clinical study

The patient characteristics are listed in Table 1.

First, we assessed the reproducibility of the quantitative values by calculating the ICC and with the Bland–Altman plots. The ICC of the SBR was 0.995 (95% CI 0.993–0.996) in the right striatum and 0.994 (95% CI 0.992–0.996) in the left striatum. The ICC of the FD was 0.999 (95% CI 0.998–0.999) in the right striatum and 0.998 (95% CI 0.997–0.998) in the left striatum. The ICCs for inter-observer variability demonstrated excellent reproducibility of both the values, SBR and FD.

Fig. 4 The Bland–Altman plots of the SBR and FD values. The mean difference was -0.002 (95% LOA; -0.323 to 0.319) for SBR and -0.004 (95% LOA; -0.132 to 0.124) for FD. The 95% LOA was narrower for FD than for SBR, implying a lower variability for FD. SBR specific binding ratio, FD fractal dimension, LOA limits of agreement

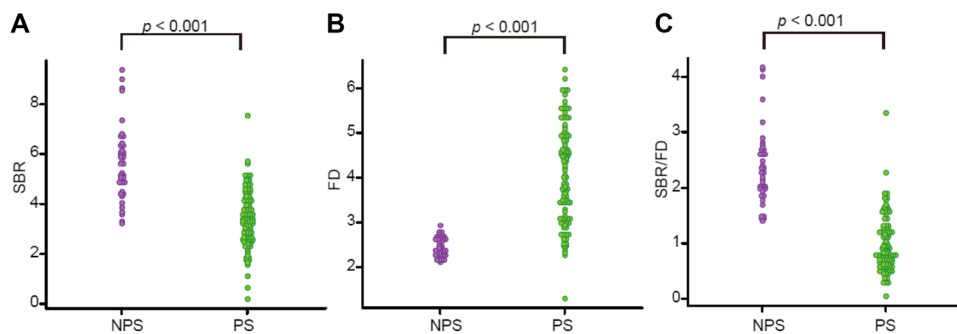
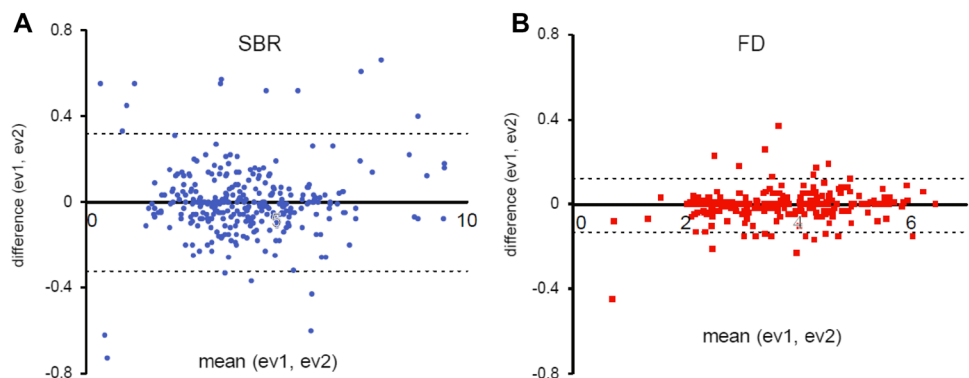


Fig. 5 Beeswarm plots of SBR, FD, and SBR/FD. All three quantitative values could be statistically divided into the two groups by the Mann–Whitney test. **a** SBR: 3.41 ± 1.11 vs 5.64 ± 1.49 , $p < 0.001$, **b**

The Bland–Altman plots of both the values are shown in Fig. 4, where the dashed lines represent the 95% limit of agreement (LOA), which is a measure of variability. We found good agreement in repeated studies for both the values; the mean difference was -0.002 (95% LOA; -0.323 – 0.319) for SBR and -0.004 (95% LOA; -0.132 to 0.124) for FD. Furthermore, the variability was smaller for FD than for SBR.

Figure 5 is the Beeswarm plots of the FD, SBR, and SBR/FD values. There were significant differences between the PS and NPS group in each value, based on the results of the Mann–Whitney test.

The mean SBR of patients with PS was significantly lower than that of patients in the NPS group (3.41 ± 1.11 vs 5.64 ± 1.49 ; $p < 0.001$; Fig. 5a), while the mean FD was significantly higher for the PS compared to the NPS group (4.06 ± 1.07 vs 2.45 ± 0.22 ; $p < 0.001$; Fig. 5b). The mean SBR/FD of patients with PS was lower than that of those in the NPS group (0.96 ± 0.49 vs 2.37 ± 0.70 ; $p < 0.001$; Fig. 5c).

In the ROC analysis, the AUCs for SBR, FD, and SBR/FD were 0.899, 0.943, and 0.964, respectively (Fig. 6a). The combined use of SBR and FD enabled a more accurate diagnosis than the use of SBR alone ($p < 0.001$).

FD: 4.06 ± 1.07 vs 2.45 ± 0.22 , $p < 0.001$, **c** SBR/FD: 0.96 ± 0.49 vs 2.37 ± 0.70 , $p < 0.001$. SBR specific binding ratio, FD fractal dimension, PS Parkinsonian syndrome, NPS non Parkinsonian syndrome

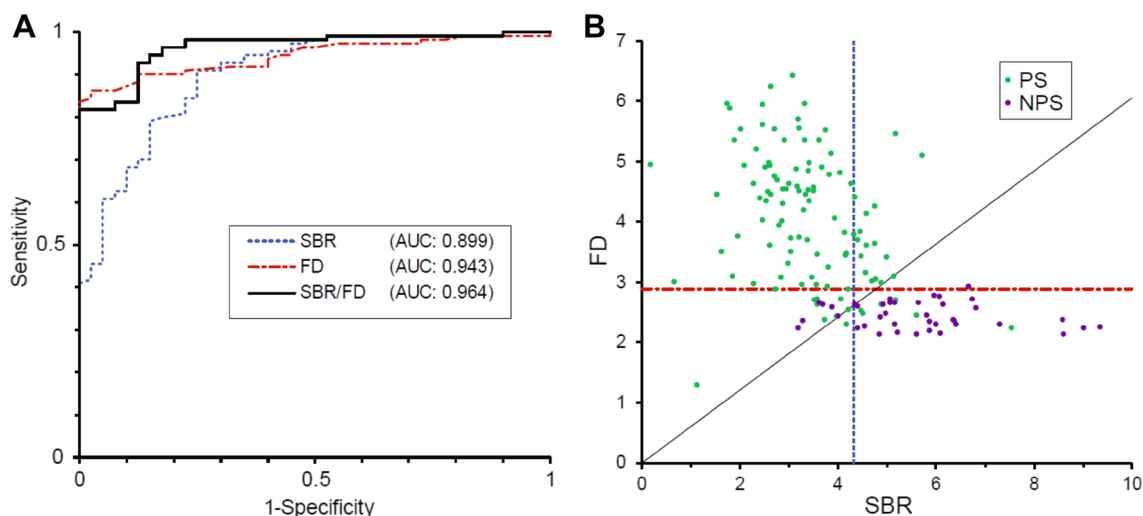


Fig. 6 ROC analysis of the SBR, FD, and SBR/FD values (**a**) and the scatter plots of the PS and NPS cases (**b**). **a** AUCs for SBR, FD, and SBR/FD were 0.899, 0.943, and 0.964, respectively. The combined use of SBR and FD enabled a more accurate diagnosis than the use of SBR alone ($p < 0.001$). **b** The cut-off values derived from ROC

analysis were 4.31 for SBR, 2.89 for FD, and 1.65 for SBR/FD. The oblique line represents the cut-off value of SBR/FD. *SBR* specific binding ratio, *FD* fractal dimension, *ROC* receiver-operating characteristics, *AUC* area under the curve, *PS* Parkinsonian syndrome, *NPS* non Parkinsonian syndrome

Table 2 Sensitivity, specificity, accuracy and AUC of the quantitative values

	Sensitivity (%)	Specificity (%)	Accuracy (%)	AUC
SBR	79.1 (87/110)	85.0 (34/40)	80.7 (121/150)	0.899
FD	84.5 (93/110)	97.5 (39/40)	88.0 (132/150)	0.943
SBR/FD	92.7 (102/110)	87.5 (35/40)	91.3 (137/150)	0.964

AUC area under the curve, *SBR* specific binding ratio, *FD* fractal dimension

The cut-off values of SBR, FD, and SBR/FD were 4.31, 2.89, and 1.65, which were derived from the ROC analysis. The sensitivity, specificity, and accuracy values were calculated using these cut-off values. The sensitivity, specificity, and accuracy of SBR were 79.1, 85.0, and 80.7%, respectively; those of FD were 84.5, 97.5, and 88.0%, respectively; and those of SBR/FD were 92.7, 87.5, and 91.3%, respectively (Table 2).

At an SBR cut-off value of 4.31, 6 false-positive cases and 23 false-negative cases were detected, for the 150 patients. At an FD cut-off value of 2.89, 1 false-positive case and 17 false-negative cases were found (Fig. 6b).

Of the 150 patients, 6 showed false-negative values for both FD and SBR. However, FD and SBR yielded different results for 35 cases; the SBR yielded correct results in 12 cases and the FD in 23 cases. Of these 35 cases, 28 were diagnosed correctly with an improved accuracy when we used the SBR/FD index. Figure 7 shows a representative case with a discrepancy between the SBR and FD values. In the visual assessment, a dot pattern was observed in bilateral

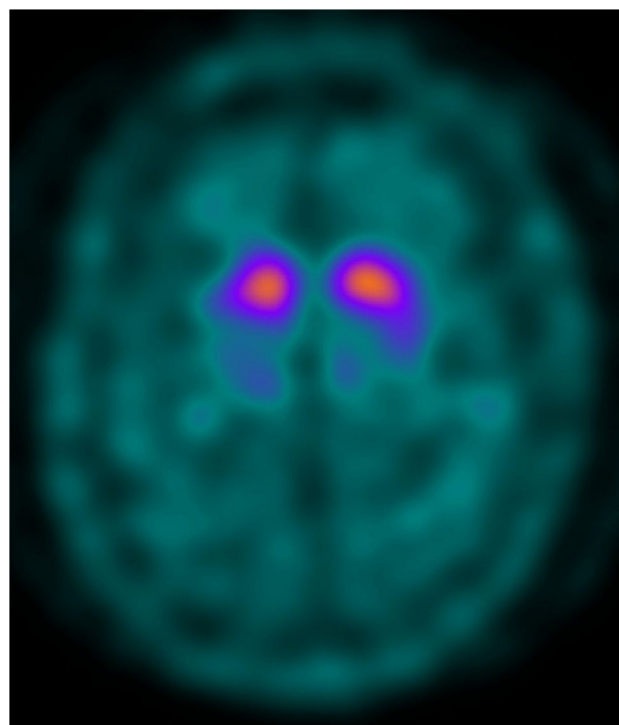


Fig. 7 A case with differences in results of the SBR and FD. FD values (3.05[R], 3.42[L]) and SBR/FD values (1.64[R], 1.70[L]) were compatible with the visual interpretation, while SBR values (4.99[R], 5.82[L]) were inconsistent. *SBR* specific binding ratio, *FD* fractal dimension, *R* right, *L* left

striatum, indicating neurodegeneration. The FD values were 3.05 in the right striatum and 3.42 in the left striatum, and the SBR/FD values were 1.64 in the right striatum and 1.70 in the left striatum, which was concordant with the visual interpretation. However, the SBR values for both the sides of the striatum were within normal limits. In this case, there is a mismatch between the results of the two values, SBR and FD; the incorrect result from the SBR value was presumably owing to the effect of brain atrophy.

Discussion

The results of this study revealed that the FD value was useful as a diagnostic index with DAT SPECT assessments. Furthermore, the combined use of SBR and FD is more effective than the use of each parameter separately. The AUC of FD was higher than that of SBR (AUC: 0.943 vs 0.899, respectively). The combined value of SBR and FD (SBR/FD) provided the most accurate result (AUC: 0.964), and there was significant difference compared to the SBR analysis ($p < 0.001$). This finding suggests that the combined use of SBR and FD will be useful in routine clinical use.

The SBR value simply reflects the tracer concentration of the striatum, while the FD value reflects the tracer distribution. Therefore, we expected that these two values, which quantify complementary aspects, improve the diagnostic accuracy when used in combination. In our clinical study, most of the false-positive or false-negative cases were different for SBR-based and FD-based diagnosis (Fig. 6b). Figure 7 shows a representative case with a discrepancy between the SBR and FD values.

To our knowledge, this is the first report to quantify the distribution of DAT SPECT uptake in the striatum using three-dimensional FD value. FD is used to evaluate the spatial heterogeneity of various types of images and previous studies have shown the utility of this method in the assessment of medical images [21]. Kuikka et al. have previously attempted to use FD to assess SPECT imaging of the striatum [22–24]. However, their fractal method measured an aspect that was completely different from the FD index used in our study. In their method, $M(\epsilon)$ was the relative dispersion (i.e., the standard deviation divided by the mean), and ϵ was the number of subregions, while $M(\epsilon)$ is the number of pixels above threshold, and ϵ is the threshold value in our study. We also found a study to have evaluated the utility of fractal analysis in DAT SPECT [25, 26], whose detail is unknown.

We consider the FD value, which is derived with this modified method, would represent the distribution of the RI accumulation and this modified method would be more suitable for quantifying SPECT imaging with low spatial resolution. Several previous reports [8–13] also demonstrated the

utility of this modified method in quantifying other types of SPECT imaging such as cerebral blood flow or lung perfusion imaging. This is the reason why we applied this method in this study. Our result demonstrated that the FD value was increased in the PS group compared with NPS group. We suppose this difference is caused by the difference of non-uniformity in striatum uptake; RI uptake in the striatum is high and homogeneous in the case of NPS patients, whereas in the case of PS patients, it presents a heterogeneous low accumulation.

We used the 3D-FA method proposed by Nagao et al. [8–13], as it is simple and provides for easy calculation of the spatial distribution of the entire 3D striatum images. This method does not require supplemental morphological imaging such as the CT or MRI; the FD value can be calculated easily using the SPECT image alone. Some of the previously proposed methods require morphological imaging for anatomical standardization [27, 28].

We used the same VOI as previously proposed by Tossici-Bolt et al. [5], which reduced inter-observer variability and enabled us to obtain FD and SBR simultaneously. For calculating the FD value, we defined two VOIs for the striatum in this method. Not requiring a use of other VOIs for background measurement reduces the inter-observer variability considerably, as seen in the results of ICC and Bland–Altman plots (Fig. 4). Furthermore, automation will enable the simultaneous measurement of SBR and FD requiring only the setting of bilateral striatal VOIs. Another merit of using this VOI is that it is suitable for the 3D-FA method. The background activity that is less than the 40% threshold would have little effect on the FD value. Accordingly, we speculate that FD value will not vary greatly by changing VOI size or shape if its size is enough large to encompass the whole striatum uptake. The Tossici-Bolt's VOI has a wide area surrounding the whole striatum. This is the reason why we applied this VOI to the 3D-FA analysis.

This study had the following limitations. First, the diagnosis of PS was clinically, not pathologically, based. A meta-analysis [29] have reported that the pooled diagnostic accuracy of PD was 82.7% (95% CI 62.6–93%) on the basis of UK Parkinson's Disease Society Brain Bank Research Center criteria. This error rate would have an influence on our results. Second, we did not assess the influence of the differences in the reconstruction parameters including scatter or attenuation correction, collimator types or the equipment on the FD value. A previous study has demonstrated the impact of reconstruction and scanner characterization on the diagnosis of SBR value [30]. We consider FD would be also influenced by these factors as with SBR. However, we think theoretically that FD value may be less influenced by the background counts compared with the case of SBR. This is because we set the threshold within the VOI for FD calculation. Further studies are needed. Third, FD estimations

may be inappropriate in cases where striatal uptakes are very low and almost equivalent to the background uptake. In such cases, fractal property may not hold, or the defined thresholds may be inappropriate. Hence, the correlation coefficient of the regression line in the fractal analysis needs to be considered to confirm whether the FD value is appropriate, although almost all the FD values calculated in this study resulted in a linear regression fit value (r^2) of 0.9 or greater.

Conclusion

Our phantom and clinical studies revealed that the FD is a useful diagnostic index in the assessment of DAT SPECT images. For a more accurate diagnosis in routine clinical examinations, a combination of the FD and SBR values (SBR/FD) is recommended.

Acknowledgements The authors thank the staff of the Division of Nuclear Medicine at the Department of Diagnostic Radiology, for their valuable support. We also thank Editage for English language editing.

Funding This research did not receive any specific grant from funding agencies in the public, commercial, or not-for-profit sectors.

Compliance with ethical standards

Conflict of interest The authors declare that they have no conflict of interest.

Ethical approval All procedures performed in studies involving human participants were in accordance with the ethical standards of the institutional and/or national research committee and with the 1964 Helsinki declaration and its later amendments or comparable ethical standards. This article does not contain any studies with animals performed by any of the authors.

Informed consent For this type of study, formal consent is not required.

References

- Vlaar AM, van Kroonenburgh MJ, Kessels AG, Weber WE. Meta-analysis of the literature on diagnostic accuracy of SPECT in parkinsonian syndromes. *BMC Neurol*. 2007;7:27.
- McKeith I, O'Brien J, Walker Z, Tatsch K, Booij J, Darcourt J, et al. Sensitivity and specificity of dopamine transporter imaging with ^{123}I -FP-CIT SPECT in dementia with Lewy bodies: a phase III, multicentre study. *Lancet Neurol*. 2007;6:305–13.
- Kwak Y, Müller ML, Bohnen NI, Dayalu P, Seidler RD. Effect of dopaminergic medications on the time course of explicit motor sequence learning in Parkinson's disease. *J Neurophysiol*. 2010;103:942–9.
- Tondeur MC, Hambye AS, Dethy S, Ham HR. Interobserver reproducibility of the interpretation of I-123 FP-CIT single-photon emission computed tomography. *Nucl Med Commun*. 2010;31:717–25.
- Tossici-Bolt L, Hoffmann SM, Kemp PM, Mehta RL, Fleming JS. Quantification of [^{123}I]FP-CIT SPECT brain images: an accurate technique for measurement of the specific binding ratio. *Eur J Nucl Med Mol Imaging*. 2006;33:1491–9.
- Varrone A, Dickson JC, Tossici-Bolt L, Sera T, Asenbaum S, Booij J, et al. European multicentre database of healthy controls for [^{123}I] FP-CIT SPECT (ENC-DAT): age-related effects, gender differences and evaluation of different methods of analysis. *Eur J Nucl Med Mol Imaging*. 2013;40:213–27.
- Nonokuma M, Kuwabara Y, Hida K, Tani T, Takano K, Yoshimitsu K. Optimal ROI setting on the anatomically normalized I-123 FP-CIT images using high-resolution SPECT. *Ann Nucl Med*. 2016;30:637–44.
- Nagao M, Murase K, Yasuhara Y, Ikezoe J. Quantitative analysis of pulmonary emphysema: three-dimensional fractal analysis of single-photon emission computed tomography images obtained with a carbon particle radioaerosol. *Am J Roentgenol*. 1998;171:1657–63.
- Nagao M, Murase K, Ichiki T, Sakai S, Yasuhara Y, Ikezoe J. Quantitative analysis of technegas SPECT: evaluation of regional severity of emphysema. *J Nucl Med*. 2000;41:590–5.
- Nagao M, Murase K. Measurement of heterogeneous distribution on Technegas SPECT images by three-dimensional fractal analysis. *Ann Nucl Med*. 2002;16:369–76.
- Nagao M, Murase K, Kikuchi T, Ikeda M, Nebu A, Fukuhara R, et al. Fractal analysis of cerebral blood flow distribution in Alzheimer's disease. *J Nucl Med*. 2001;42:1446–50.
- Nagao M, Sugawara Y, Ikeda M, Fukuhara R, Hokoishi K, Murase K, et al. Heterogeneity of cerebral blood flow in frontotemporal lobar degeneration and Alzheimer's disease. *Eur J Nucl Med Mol Imaging*. 2004;31:162–8.
- Nagao M, Sugawara Y, Ikeda M, et al. Heterogeneity of posterior limbic perfusion in very early Alzheimer's disease. *Neurosci Res*. 2006;55:285–91.
- Söderlund TA, Dickson JC, Prvulovich E, Ben-Haim S, Kemp P, Booij J, et al. Value of semiquantitative analysis for clinical reporting of ^{123}I -2- β -carbomethoxy-3 β -(4-iodophenyl)- N -(3-fluoropropyl)nortropane SPECT studies. *J Nucl Med*. 2013;54:714–22.
- Mäkinen E, Joutsa J, Johansson J, Mäki M, Seppänen M, Kaasinen V. Visual versus automated analysis of [^{123}I]FP-CIT SPECT scans in parkinsonism. *J Neural Transm (Vienna)*. 2016;123:1309–18.
- Booij J, Dubroff J, Pryma D, Yu J, Agarwal R, Lakhani P, et al. Diagnostic performance of the visual reading of ^{123}I -Ioflupane SPECT images when assessed with or without quantification in patients with movement disorders or dementia. *J Nucl Med* 2017. <https://doi.org/10.2967/jnumed.116.189266> (Epub ahead of print).
- Nicastro N, Garibotto V, Allali G, Assal F, Burkhard PR. Added value of combined semi-quantitative and visual [^{123}I]FP-CIT SPECT analyses for the diagnosis of dementia with Lewy Bodies. *Clin Nucl Med*. 2017;42(2):e96–e102.
- Schneider CA, Rasband WS, Eliceiri KW. NIH Image to ImageJ: 25 years of image analysis. *Nat Methods*. 2012;9:671–5.
- Bland JM, Altman DG. Statistical methods for assessing agreement between two methods of clinical measurement. *Lancet*. 1986;327:307–10.
- DeLong ER, DeLong DM, Clarke-Pearson DL. Comparing the areas under two or more correlated receiver operating characteristic curves: a nonparametric approach. *Biometrics*. 1988;44:837–45.
- Michaliek F, Dewey M. Fractal analysis in radiological and nuclear medicine perfusion imaging: a systematic review. *Eur Radiol*. 2014;24:60–9.

22. Kuikka JT, Tiihonen J, Karhu J, Bergström KA, Räsänen P. Fractal analysis of striatal dopamine re-uptake sites. *Eur J Nucl Med*. 1997;24:1085–90.
23. Kuikka JT, Yang J, Karhu J, Laitinen T, Tupala E, Hallikainen T, et al. Imaging the structure of the striatum: a fractal approach to SPECT image interpretation. *Physiol Meas*. 1998;19:367–74.
24. Kuikka JT, Tiihonen J, Bergström KA, Karhu J, Räsänen P, Eronen M. Abnormal structure of human striatal dopamine re-uptake sites in habitually violent alcoholic offenders: a fractal analysis. *Neurosci Lett*. 1998;253:195–7.
25. Bolt L, Fleming JS, Kemp PM. The 3D fractal dimension of DaTSCAN Images. *Nucl Med Commun*. 2006;27:296 (**abstract**).
26. Bolt L, Fleming JS, Kemp PM. Quantifying DaTSCAN TM images- a comparison of region-of-interest and fractal analysis. *Eur J Nucl Med Mol Imaging*. 2006;33:S98 (**abstract**).
27. Yokoyama K, Imabayashi E, Sumida K, Sone D, Kimura Y, Sato N, et al. Computed-tomography-guided anatomic standardization for quantitative assessment of dopamine transporter SPECT. *Eur J Nucl Med Mol Imaging*. 2017;44:366–72.
28. Kim JS, Cho H, Choi JY, Lee SH, Ryu YH, Lyoo CH, et al. Feasibility of computed tomography-guided methods for spatial normalization of dopamine transporter positron emission tomography image. *PLoS One*. 2015;10(7):e0132585. <https://doi.org/10.1371/journal.pone.0132585>.
29. Rizzo G, Copetti M, Arcuti S, Martino D, Fontana A, Logroscino G. Accuracy of clinical diagnosis of Parkinson disease: a systematic review and meta-analysis. *Neurology*. 2016;86:566–76.
30. Dickson JC, Tossici-Bolt L, Sera T, Booi J, Ziebell M, Morbelli S, et al. The impact of reconstruction and scanner characterisation on the diagnostic capability of a normal database for [123I] FP-CIT SPECT imaging. *EJNMMI Res*. 2017;7:10. <https://doi.org/10.1186/s13550-016-0253-0> (**Epub 2017 Jan 24**).